Tracking indices as measures of synchronization of isotopic temperature of NZ abalone shells with ambient water temperature

[1]**Kim, S.W. and** [1]**I.L. Hudson**

[1]School of Mathematics and Statistics
University of South Australia, GPO Box 2471, Adelaide, SA 5000, Australia.
E-Mail: kimsw001@students.unisa.edu.au

Keywords: *synchrony, kernel smoothing, tracking index, bootstrapping, growth*

ABSTRACT

Synchrony, synchronistic occurrence, has been studied in population dynamics, health science and in phenology. Moran (1953) first introduced the concept of synchrony between population dynamics and concomitant weather conditions using Canadian lynx data showing that the degree of synchrony decreases with increasing distance and since then, it has been studied in various areas of research. Although spatial synchrony, which considers similarity across locations and species, has been studied widely, temporal synchrony, which considers timing of events, has been studied mostly in phenology.

In a recent study, Naylor et al. (2007) suggested the possible use of variations in the ratios of oxygen and carbon isotopes to determine age, growth and reproductive patterns in shells of *Haliotis iris*. They suggested that oxygen isotope profiles within shells reflected ambient water temperature at the time of shell precipitation, and that these (δ^{18}O and δ^{13}C) profiles could be used to determine age and growth patterns. Naylor et al. (2007) used two temperature series, ambient water temperature and isotopic temperature from shells. Their preliminary work indicated that two types of growth model, the von-Berterlanffy (VB) or the Gompertz (G) growth model were equally good in "mirroring" isotopic temperature. However, the G model was preferred to the VB model as it fitted better to tagging information data (Naylor et al. 2007).

In this study, we look at the tracking indices of two temperature series, ambient water temperature and isotopic temperature of Naylor et al. (2007) to measure synchronicity. We show that temperature estimated from abalone shells using oxygen isotope profiles statistically track and/or synchronize with ambient water temperature. In terms of fitting isotopic temperature with ambient water temperature, one growth model, namely the von Berterlanffy (VB), fits significantly better than the G model. This is established using a block bootstrapping method to calculate the confidence interval of so the so-called tracking indices, that mirror synchrony.

This work represents an improvement because the VB model and the G model, by their definition, give different biomass estimation for the future in terms of time and amount. The VB model will estimate smaller biomass than the G model, although the G model will take longer to build the available biomass, since it reaches the minimum legal size 2-6 years later than the VB model. By choosing the VB model over the G model, we are selecting a model where in a shell reaches the minimum legal size faster, although the biomass of the shell is not as heavy as the amount calculated via the G model. The impact on total biomass, in the future, via the VB and the G models was not examined in this study, and is future work.

Tracking indices between two temperature series (isotopic - estimated shell temperature and ambient water temperature) were obtained for four shells: (a) between the two temperature series as they are, (b) between ambient water temperature and the kernel smoothed isotopic temperature; and (c) on the moving block bootstrapped series of isotopic temperature and ambient water temperature.

The local bandwidth choice in Kernel regression showed the largest bandwidth of shell 3, which can be related to the smallest asymptotic length (L_∞=136.32 with VB) and slower growth rate (large K, K=0.38 with VB) and the smallest bandwidth of shell 2, which can be related to the largest asymptotic length (L_∞=181.84 with VB) and its fast growth rate to the minimum legal size (Naylor et al. 2007). At the minimum legal size, shell 3 will be 6.6 years old whereas shell 2 will only be 4.4 years old.

Tracking indices showed that the shell and water temperature series are synchronizing and parallel; and that the VB growth model synchronizes significantly better for shells 1, 3, and 4. The G growth model synchronizes significantly better for shell 2 only.

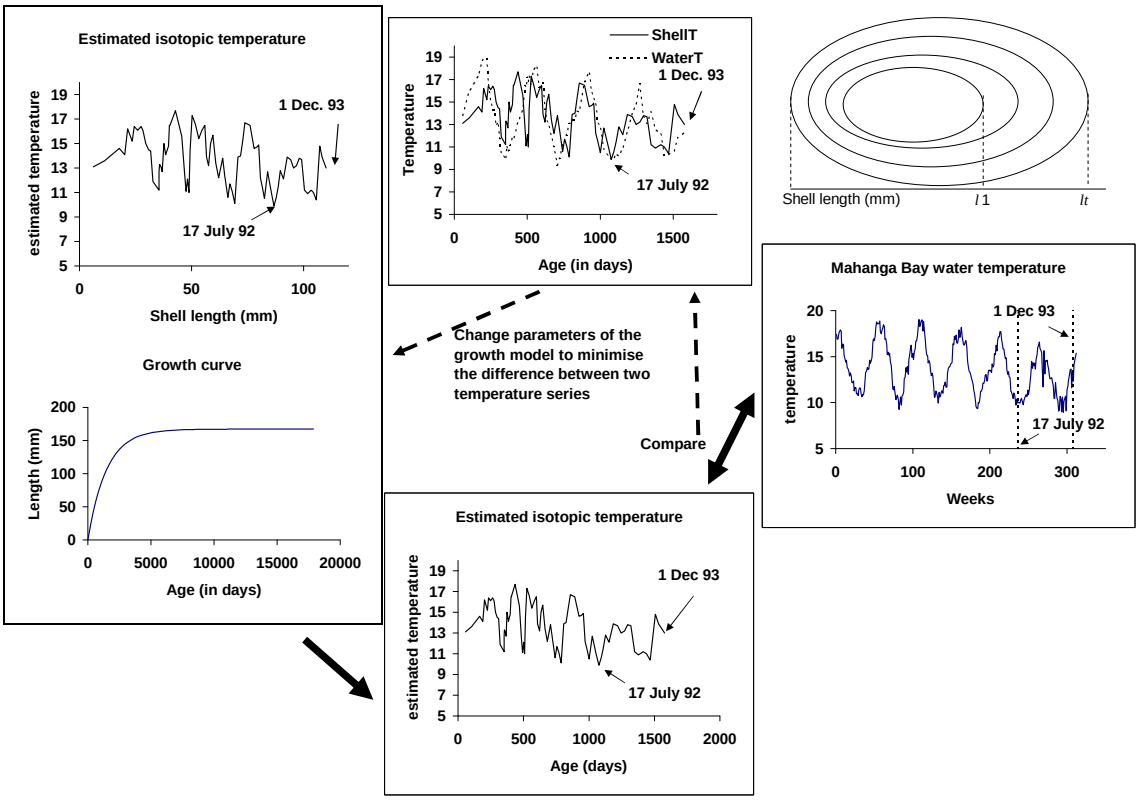

Figure 1. Schema of modelling and estimation.

1 INTRODUCTION

Synchrony has been studied in population dynamics (Moran 1953, Ranta et al. 1995a, 1995b, 1997, Bjørnstad 2000, Bjørnstad et al. 1999a, 1999b, Økland and Bjørnstad 2003, Koenig 2002, Liebhold et al. 2004, Raimondo et al. 2004), health science (Cummings et al. 2004, Basarsky et al. 1998) and in phenology (Augspurger 1983, Keatley et al. 2004, Hudson et al. 2006). Moran (1953) first introduced the concept of synchrony between population dynamics and concomitant weather conditions using the Canadian lynx data. He showed that the degree of synchrony decreases with increasing distance (i.e. the lynx cycle was less synchronous with temperature from areas which are more distant). Since then, synchronicity between population dynamics and weather is known as the "Moran effect". Although spatial synchrony, which considers similarity across locations and species, has been studied widely (Ranta et al. 1995b, Bjørnstad 2000, Bjørnstad et al. 1999a, 1999b, Økland and Bjørnstad 2003, Koenig 2002, Liebhold et al. 2004, Raimondo et al. 2004), temporal synchrony, which considers timing of events, has been studied mostly in phenology (Keatley et al. 2004, Augspurger 1983, Hudson et al. 2006).

In a recent study, Naylor et al. (2007) suggested the possible use of variations in the ratios of oxygen and carbon isotopes to determine age, growth and reproductive patterns in shells of *Haliotis iris*. They suggested that oxygen isotope profiles within shells reflected ambient water temperature at the time of shell precipitation, and that these (δ^{18}O and δ^{13}C) profiles could be used to determine age and growth patterns. Naylor et al. (2007) used two temperature series, ambient water temperature and isotopic temperature from shells. To match these two temperature series, an age at each shell incremental length was estimated using the two growth models, VB and G, and the tagging information, shell lengths at the time of tagging and recapturing (Figure 1). The approach adopted here is to match estimated shell temperature at length (L) with ambient water temperature at chronological time - essentially, matching two different time metameters and two different functionals. Naylor et al.'s (2007) preliminary work indicated that two types of growth model, the von-Berterlanffy (VB) or the Gompertz (G) growth model were equally good in "mirroring" isotopic temperature. However, the G model was preferred to the VB model because it fitted better to fisheries tagging information data.

In this study, we use synchronicity as a measure of goodness of fit. We look at the tracking indices of two temperature series, ambient water temperature and isotopic temperature of Naylor et al. (2007) to assess synchronicity.

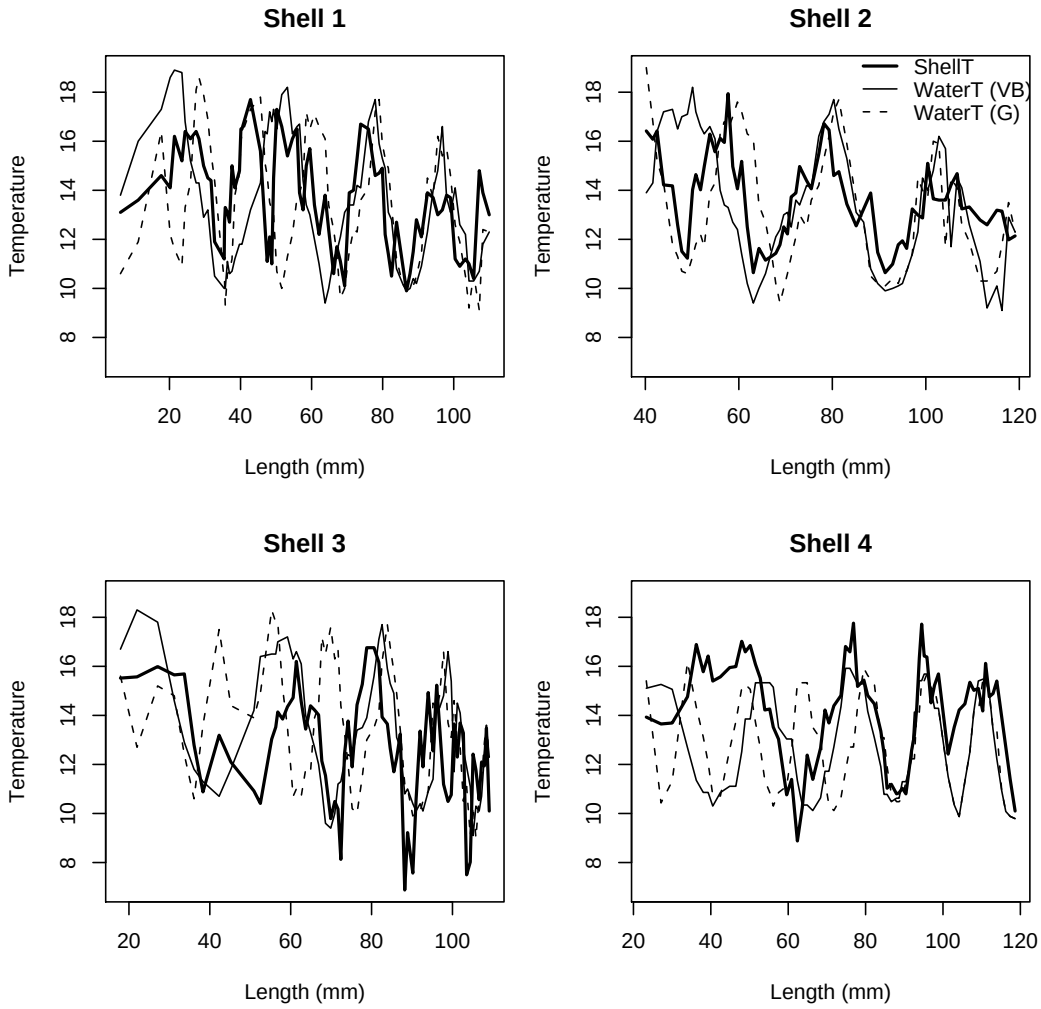

Figure 2. Fitted ambient water temperature via the von Berterlanffy (WaterT (VB), thin solid line) and the Gompertz (WaterT (G), dashed line) model and isotopic temperature (ShellT, think solid line) for each shell. This shell was tagged on 17th July 1992 and recaptured on 1st December 1993.

2 DATA AND MODELS

Temperature series from two sources, ambient water temperature (mean weakly temperature records from Mahanga Bay and for Cape Campbell (Naylor et al. 2007) and mean monthly ambient water temperatures estimates NIWA SST Archive (Uddstrom and Oien 1999)) estimated isotopic temperature from four shells were used for this study. Four shells from two localities in New Zealand were used; three shells from Mahanga Bay and one (shell 4) from Cape Campbell (Naylor et al. 2007). Ambient water temperature has been fitted to the estimated isotopic temperature series using two growth models: von Berterlanffy (VB) and Gompertz (G) (Naylor et al. 2007). The data used for this study, fitted ambient water temperature via the Von Beterlanffy and the Gompertz growth model. This with isotopic temperature are shown in Figure 2 for the four shells.

For the age-based von Berterlanffy growth model, with three parameters, asymptotic length, L_∞, rate parameter, K, and initial time parameter, t_0. The expected length at day t, l_t, is calculated as:

$$l_t = L_\infty \left(1 - e^{-\frac{K(t-t_0)}{365}}\right). \quad (1)$$

Equation (1) can be rearranged to obtain the expected age in days, $\hat{t}_{l_i}$, of abalone of length l_i, where:

$$\hat{t}_{l_i} = t_0 - \frac{365}{K} \ln\left(1 - \frac{l_i}{L_\infty}\right), \quad (2)$$

the expected growth increment $\hat{d}$, n days after tagging at l_1 is:

$$\hat{d} = (L_\infty - l_1)\left(1 - e^{-\frac{nK}{365}}\right). \quad (3)$$

Note that under the von-Berterlanffy growth model, a shell grows fast when it is small, but slows down its growth rate as it becomes larger (Figure 3).

For the age-based Gompertz growth model, with three parameters, asymptotic length, $L_\infty^{'}$, rate parameter,

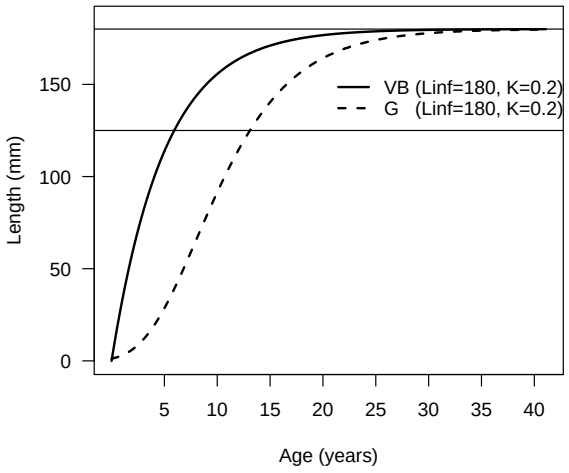

Figure 3. Von Berterlanffy (VB) growth curve and Gompertz (G) growth curve. Linf:L_∞

$K^{'}$, and initial time parameter, $t_0^{'}$. The expected length at day t, l_t, is calculated as:

$$l_t = L_\infty^{'} e^{-\frac{1}{K'}\exp\left(-\frac{K^{'}(t-t_0^{'})}{365}\right)}. \quad (4)$$

The latter equation can be rearranged to get the expected age in days, $\hat{t}_{l_i}$ of an abalone of length l_i:

$$\hat{t}_{l_i} = t_0^{'} - \left(\frac{365}{K'}\right)\ln\left(-K^{'}\ln\left(\frac{l_i}{L_\infty^{'}}\right)\right). \quad (5)$$

The expected growth increment ratio, $\hat{r}$, n days after the abalone is tagged at l_1 is then:

$$\hat{r} = \left(\frac{l_1}{L_\infty^{'}}\right)^{\exp\left(\frac{-nK}{365}\right)-1}. \quad (6)$$

Under the Gompertz growth model, a shell begins at a slow growth rate, but then accelerates its growth rate after a certain size. Its growth rates then decreases as it becomes larger (Figure 3).

The VB growth model allows a shell to grow fast when its size is small so it makes shells reach their minimum legal size sooner than using the G model, which makes shells grow very slow when their sizes are small. However, the asymptotic length is much larger when the G growth model is used than when the VB model is used. Hence, although the VB model makes abalones available to the fisheries (i.e. when it reaches the minimum legal size) 2-6 years sooner than G model, the biomass available to the fishery using G model will be larger than those using VB model because shells grow larger.

The shells' estimated ages ranged from 4 to 6 years using the VB model and from 6 to 12 years via the G model. It has to be noted that shell 2 was younger (4.4 years *vs* 5.5-6.6 years for shells 1, 3, and 4 (via the VB) and 6.6 years *vs* 8.9-12.0 years for shells 1, 3, and 4 (via the G model)).

3 STATISTICAL METHODS

3.1 Kernel Smoothing

Isotopic shell temperature is first smoothed using a local linear kernel regression (Wand and Jones 1995). Kernel smoothing estimates the underlying function without specification of a parametric model.

Let $\hat{T}_1$, $\hat{T}_2$, ..., $\hat{T}_n$ be the estimated isotopic temperature over length $(0, L)$. Assuming the estimated isotopic temperature includes error, we have the following model:

$$\hat{T}_l = \mu_l + \varepsilon_l, \quad (7)$$

where μ_l is the underlying mean isotopic temperature at length l and ε is an error with mean of zero. For $l \in L$, we estimate μ_l using local linear kernel regression with a compact kernel. Centering the kernel at l, let $\hat{T}_{[1]}$, $\hat{T}_{[2]}$, ..., $\hat{T}_{[m]}$ be the observations that are within the support of the kernel. The estimate $\hat{\mu}_l$ for equation (7) is defined as:

$$\hat{\mu}_l = \sum_{i=1}^{m} \omega_i(l)\hat{T}_{[i]}, \quad (8)$$

where

$$\omega_i(t) = \frac{\hat{s}_2(l;h) - \hat{s}_1(l;h)(l_{[i]} - l)K_h(l_{[i]} - l)}{\hat{s}_2(l;h)\hat{s}_0(l;h) - \hat{s}_1(l;h)^2}, \quad (9)$$

$$\hat{s}_r(l;h) = \sum_{i=1}^{m}(l_{[i]} - l)^r K_h(l_{[i]} - l), \quad (10)$$

and $l_{[1]}, l_{[2]}, ..., l_{[m]}$ are the length indices corresponding to $\hat{T}_{[1]}$, $\hat{T}_{[2]}$, ..., $\hat{T}_{[m]}$, and $K_h(l_{[i]} - l)$ is the kernel function centered about point l with bandwidth h (Wand and Jones 1995).

Note that an excessively narrow bandwidth results in an under-smoothed estimate which removes little of the random fluctuations from the underlying data. An over-sized bandwidth on the other hand results in an over-smoothed estimate that removes part of the underlying structure.

We examined both the global (a fixed bandwidth for the overall series) and local (a flexible bandwidth for the overall series) bandwidth for kernel smoothing.

3.2 Tracking Index

Chase et al. (2004) defined a tracking index (TI) as:

$$TI = \left\{ 1 - \frac{\sum_{i=1}^{n} \left| T_i - \hat{T}_i \right|}{\sum_{i=1}^{n} \hat{T}_i} \right\} \times 100, \qquad (11)$$

with $\hat{T}_i$ given by equation (7).

We employed TI to test synchronization of the estimated isotopic and ambient water temperature profiles for a given shell separately. TI indicates how well fitted ambient water temperature (T_i) follows its isotopic temperature ($\hat{T}_i$) over the entire time series. A tracking index TI=100 represents perfect tracking, that is ambient water temperature perfectly matches isotopic temperature. For the tracking index variant which uses a kernel smoothed isotopic temperature, $\hat{\mu}_l$, is substituted for isotopic temperature ($\hat{T}_i$) in equation (11).

3.3 Moving block bootstrap test

To obtain the significance of and confidence interval for the tracking index (TI), the moving block bootstrap is used (Efron and Tibshirani 1993 and Chase et al. 2004). A total of $n = 1000$ bootstrap samples are generated for each recorded shell. A tracking index, as defined in equation (11), can then be calculated for each bootstrap sample, providing a collection of 1000 values of the tracking index, TI_{1-1000}, for each recorded shell. The median tracking index and its 95% confidence interval, can then be calculated for each shell (Hettmansperger and McKean 1998).

Note that a block size l, in the moving block bootstrap test needs to be large enough to have observations more than l time units apart nearly independent, but must still retain the correlation present in observations less than l units apart. A block length l of 10 units for shells 1 and 3, 11 units for shell 2, and 9 units for shell 4, was selected for use in this application (Chase et al. 2004).

4 RESULTS

4.1 Kernel smoothing

The bandwidth for kernel smoothing with a global bandwidth is shown in Table 1. The global bandwidth lay within the local bandwidth range. Both kernel smoothing fit well to the actual isotopic temperature. Kernel smoothing with local bandwidth fits isotopic temperature slightly better than global, but not significantly at the α=0.05 level (Table 1).

Table 1. Global bandwidth and range of local bandwidth for each shell for kernel smoothing.

	global bandwidth		local bandwidth	
Shell	h	r^2	h (range)	r^2
1	2.889	0.821	(1.778, 6.257)	0.865
2	2.887	0.878	(2.177, 4.017)	0.893
3	3.998	0.670	(2.608, 9.915)	0.745
4	3.260	0.915	(2.113, 5.549)	0.931

Table 1 shows that shell 3 had the largest range (2.608-9.915) in local h and also had the largest global h (3.998) while shell 2 had the smallest range (2.177-4.017) in local bandwidth with smallest global h (2.887). The largest bandwidth of shell 3 can be related to the smallest asymptotic length (L_∞=136.32 with VB) and slower growth rate (large K, K=0.38 with VB) and the smallest bandwidth of shell 2 can be related to the largest asymptotic length (L_∞=181.84 with VB) and its fast growth rate to the minimum legal size (Naylor et al. 2007). At the minimum legal size, shell 3 will be 6.6 years old whereas shell 2 will only be 4.4 years old. Shell 1 had the smallest bandwidth (1.778) and shell 3 had the largest bandwidth (9.915) overall.

Kernel smoothed isotopic temperature and fitted ambient water temperature using both the VB and G models are shown in Figure 4 for shell 4.

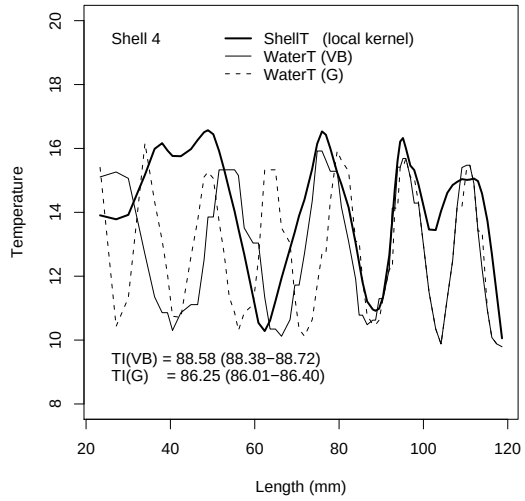

Figure 4. Kernel smoothed isotopic temperature and fitted ambient water temperature using the VB and the G models for shell 4. TI and its 95% confidence interval are shown.

Table 2. Tracking index between isotopic temperature and ambient water temperature.

	Tracking index		Tracking index using kernel smoothing			
			Global kernel		Local kernel	
Shell	TI(VB)	TI(G)	TI(VB)	TI(G)	TI(VB)	TI(G)
1	**85.12**	84.74	**86.56**	85.51	**86.33**	85.23
2	87.26	**87.67**	87.75	**88.44**	87.72	**88.43**
3	**84.56**	78.59	**87.20**	81.35	**86.69**	81.07
4	**87.66**	85.49	**88.65**	86.43	**88.55**	86.29
Shell	Median block bootstrapped TI (95% confidence limits)					
1	**85.23**	84.69	**86.67**	85.36	**86.42**	85.10
	(85.09, 85.35)	(84.60, 84.79)	(86.55, 86.81)	(85.27, 85.51)	(86.33, 86.66)	(85.02, 85.22)
2	87.34	**87.72**	87.97	**88.44**	87.94	**88.43**
	(87.26, 87.61)	(87.67, 87.79)	(87.81, 88.16)	(88.40, 88.50)	(87.74, 88.14)	(88.38, 88.48)
3	**84.55**	78.64	**87.35**	81.35	**86.78**	81.04
	(84.47, 84.59)	(78.51, 78.91)	(87.22, 87.45)	(81.11, 81.61)	(86.67, 86.91)	(80.75, 81.30)
4	**87.75**	85.32	**88.67**	86.38	**88.58**	86.25
	(87.56, 87.88)	(85.13, 85.48)	(88.48, 88.82)	(86.19, 86.56)	(88.38, 88.72)	(86.01, 86.40)

4.2 Tracking

VB and G specific tracking indices between isotopic and ambient water temperature are shown in Table 2. Tracking indices which compare ambient water temperature to isotopic temperature for the overall series show that the VB model fits isotopic temperature better for shells 1, 3, and 4 and the G model fits better for shell 2. The G model for shell 2 fits the best according to the overall tracking index (TI=87.67) and the VB model for shell 4 also fits very well (TI=87.66). Tracking indices which compare ambient water temperature to the kernel smoothed isotopic temperature (with global bandwidth for the overall series) show that the VB model for shell 4 fits the best (TI=88.65) and the G model for shell 2 follows with a TI of 88.44. Tracking indices which compare ambient water temperature to the kernel smoothed isotopic temperature is higher than tracking indices for ambient water temperature and actual isotopic temperature. The tracking indices for ambient water temperature with the kernel smoothed isotopic temperature (with local bandwidth for the overall series) show that the VB model for shell 4 fits the best (TI=88.55, Figure 4) and the G model for shell 2 follows with TI of 88.43. Tracking indices of ambient water temperature to the kernel smoothed isotopic temperature (with local bandwidth) is slightly lower than tracking indices comparing ambient water temperature to the kernel smoothed isotopic temperature with global bandwidth (Table 2).

The results from the moving block bootstrapped sample are similar but show a significant difference between the TI of the two growth models. The VB model for shell 4 fits the best (TI=87.75, 88.67, and 88.58 with the raw, the global kernel estimated, and the local kernel estimated isotopic temperature, respectively) and the G model for shell 2 follows with TIs of 87.72, 88.44, and 88.43 with the raw, the global kernel estimated, and the local kernel estimated isotopic temperature, respectively (Table 2). Note that the differences in TI between the VB model and the G model for each shell are significant at the α=0.05 level.

5 DISCUSSION

Tracking indices show that ambient water temperature fitted with both the VB and the G model fits well to isotopic temperature. The moving block bootstrapping test show that there is however a significant difference in synchronicity according to the growth models used. For shells 1, 3, and 4, the tracking indices show that ambient water temperature fitted to the isotopic temperature with the VB model synchronizes significantly better to that obtained using the G model. Only the isotopic temperature for shell 2 was synchronizing significantly better with ambient water temperature fitted with the G model than the VB model.

The main difference between the G model and the VB model is that the G model has slower growth rate at a small size than the VB model. For shell 2, it has slower growth rate than other shells at a small size and hence the isotopic temperature for shell 2 is synchronizing better with ambient water temperature fitted with the G model.

We show that temperature estimated from abalone shells using oxygen isotope profiles statistically track and/or synchronize with ambient water temperature. In terms of fitting isotopic temperature with ambient water temperature, one growth model, namely the VB model, fits significantly better than the G model using block bootstrapping method.

It should be noted that very high tracking is achieved between ambient water temperature and isotopic temperature via Naylor et al.'s (2007) method irrespective of which growth model is used.

This paper shows the utility of the tracking index (with and without kernel smoothing) and of the moving block bootstrapping method to test for synchronization. Here the value of both the VB and G growth models and the method of mapping of Naylor et al. (2007) are further demonstrated.

6 ACKNOWLEDGEMENT

We thank the NZ Ministry of Fisheries for letting us use results from the MFish funded project GEN2004-01. We also thank people involved in the GEN2004-01 project, Reyn Naylor, Babara Manighetti and Helen Neil (NIWA), for permission to investigate synchrony further.

7 REFERENCES

Augspurger, C.K. (1983), Phenology, flowering synchrony, and fruit set of six neotropical shrubs, *Biotropica* **15**, 257-267.

Basarsky,T.A., S.N. Duffy, R. David Andrew, and B.A. MacVicar (1998), Imaging Spreading Depression and Associated Intracellular Calcium Waves in Brain Slices, *The Journal of Neuroscience* **18 (18)**, 7189-7199.

Bjørnstad, O.N. (2000), Cycles and synchrony: two historical 'experiments' and one experience, *Journal of Animal Ecology* **69**, 869-873.

Bjørnstad, O.N., N.Ch. Stenseth, and T. Saitoh (1999a), Synchrony and Scaling in Dynamics of voles and mice in Nothern Japan, *Ecology* **80 (2)**, 622-637.

Bjørnstad, O.N., R.A. Ims and X. Lambin (1999b), Spatial population dynamics: analyzing patterns and processes of population synchrony, *Tree* **14 (11)**, 427-432.

Chase J.G., A.D. Rudge, G.M. Shaw, G.C. Wake, D. Lee, I.L. Hudson and L. Johnston (2004), Modeling and control of the agitation-sedation cycle for critical care patients, *Medical Engineering and Physics*, **26**, 459-471.

Cummings, D.A.T., R.A. Irizarry, N.E. Huang, T.P. Endy, A. Nisalak, K. Ungchusak and D.S. Burke (2004), Travelling waves in the occurrence of dengue haemorrhagic fever in Thailand, *Nature*, **427**, 344-347.

Efron B. and R.J. Tibshirani (1993), *An Introduction to the Bootstrap. Monographs on Statistics and Applied Probability*, London: Chapman & Hall.

Hettmansperger, T.P. and J.W. McKean (1998), *Robust nonparametric statistical methods*, London: Arnold.

Hudson, I.L., M.R. Keatley, S.W. Kim and I. Kim (2006), Synchronicity in Phenology: from PAP Moran to now, *Australian Statistical Conference/New Zealand Statistical Association (NZSA) conference, 3th - 6th, July, Auckland, NZ.*

Keatley, M.R., I.L. Hudson, and T.D. Fletcher (2004), Long-term flowering synchrony of Box-ironbark eucalypts, *Australian Journal of Botany* **52**, 47-54.

Koenig, W.D. (2002), Global patterns of environmental synchrony and the Moran effect, *Ecography* **25**, 283-288.

Liebhold, A., V.Sork, M. Peltonen, W. Koenig, O.N. Bjørnstad, R. Westfall, J. Elkinton and J.M.H. Knops (2004), Within-population spatial synchrony in masting seeding of North American oaks, *Oikos* **104**, 156-164.

Moran, P.A.P. (1953), The Statistical Analysis of the Canadian Lynx Cycle. II. Synchronization and Meteorology, *Australian Journal of Zoology* **1**, 291-298.

Naylor, J.R., B.M. Manighetti, H.L. Neil and S.W. Kim (2007), Validated estimation of growth and age in the New Zealand abalone *Haliotis iris* using stable oxygen isotopes, *Marine and Freshwater Research*, **58 (4)**, 354-362.

Økland, B. and Bjørnstad, O.N. (2003), Synchrony and geographical variation of the spruce bark beetle (*Ips typographus*) during a non-epidemic period, *Population Ecology*, **45**, 213-219.

Raimondo, S., A.M. Liebhold, J.S. Strazanac and L. Butler (2004), Population synchrony within and among Lepidoptera species in relation to weather, phylogeny, and larval phenology, *Ecological Entomology* **29**, 96-105.

Ranta, E., V. Kaitala, J. Lindström and H. Lindén (1995a), Synchrony in population dynamics, *Proceedings: Biological Sciences* **262**, 113-118.

Ranta, E., J. Lindström and H. Lindén (1995b), Synchrony in tetranoid population dynamics, *Journal of Animal Ecology* **64**, 767-776.

Ranta, E., V. Kaitala, J. Lindström, E. Helle (1997), The Moran effect and synchrony in population dynamics, *OIKOS* **78**, 136-142.

Uddstrom, M.J. and N.A. Oien (1999), On the use of high-resolution satellite data to describe the spatial and temporal variability of sea surface temperatures in the New Zealand region, *Journal of Geophysical Research*, **104**, 20729-20751.

Wand, M.P. and M.C. Jones (1995), *Kernel Smoothing*, London: Chapman & Hall.